

# Active Energy Harvesting from Microbial Fuel Cells at the Maximum Power Point without Using Resistors

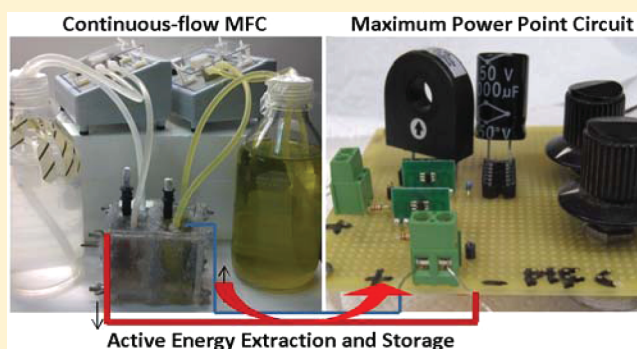
Heming Wang,<sup>†</sup> Jae-Do Park,<sup>‡</sup> and Zhiyong Ren<sup>\*,†</sup>

<sup>†</sup>Department of Civil Engineering <sup>‡</sup>Department of Electrical Engineering University of Colorado Denver, Denver, Colorado 80004, United States

**S** Supporting Information

**ABSTRACT:** Microbial fuel cell (MFC) technology offers a sustainable approach to harvest electricity from biodegradable materials. Energy production from MFCs has been demonstrated using external resistors or charge pumps, but such methods can only dissipate energy through heat or receive electrons passively from the MFC without any controllability. This study developed a new approach and system that can actively extract energy from MFC reactors at any operating point without using any resistors, especially at the peak power point to maximize energy production. Results show that power harvesting from a recirculating-flow MFC can be well maintained by the maximum power point circuit (MPPC) at its peak power point, while a charge pump was not able to

change operating point due to current limitation. Within 18-h test, the energy gained from the MPPC was 76.8 J, 76 times higher than the charge pump (1.0 J) that was commonly used in MFC studies. Both conditions resulted in similar organic removal, but the Coulombic efficiency obtained from the MPPC was 21 times higher than that of the charge pump. Different numbers of capacitors could be used in the MPPC for various energy storage requirements and power supply, and the energy conversion efficiency of the MPPC was further characterized to identify key factors for system improvement. This active energy harvesting approach provides a new perspective for energy harvesting that can maximize MFC energy generation and system controllability.



Active Energy Extraction and Storage

## INTRODUCTION

A microbial fuel cell (MFC) is a bioelectrochemical system (BES) that employs exoelectrogenic bacteria to oxidize organic matter and produce direct electrical current. Because MFC offers a sustainable solution for remote sensing and simultaneous pollution control and energy production, it has been intensively researched in recent years, and the improvements in reactor configurations, materials, and operations have led to orders of magnitude increase in power density, from less than 1 mW/m<sup>2</sup> to the level of 6.9 W/m<sup>2</sup>.<sup>1,2</sup> However, most studies operate the MFC with a static external resistance or applied potential and report the power density using a polarization curve, which assumes that the maximum power density is achieved when the applied external resistance is equal to the MFC internal resistance.<sup>3–5</sup> Such characterizations do represent the theoretical potential of MFC power output, but no usable energy could be captured, because the electricity generated in such systems is actually dissipated into heat instead of being utilized by electronics. Moreover, the fixed external resistance cannot always match the system internal resistance and recover the maximum power output during MFC operation, because the internal resistance of an MFC varies constantly with changes in microbial activities and operational parameters, such as substrate concentration, pH, and temperature.<sup>6–9</sup> Studies showed that MFCs may lose more

than 50% of produced power across the internal resistance if the operating voltage is not at the maximum power point voltage.<sup>10</sup>

To effectively and efficiently harvest MFC energy, unnecessary resistors need to be eliminated, and technologies need to be developed to track and harvest energy at the peak level with sufficient controllability. Progress has been made in maximum power point tracking (MPPT) and harvesting systems, such as using perturbation and observation or gradient method to track and optimize external resistance.<sup>5,10</sup> For example, Pinto et al. found that MFC power output can be significantly improved when real-time resistance optimization was implemented during long-term operation.<sup>5</sup> However, traditional MPPT techniques still use external resistances and cannot capture and utilize the energy directly. Another harvesting approach is using capacitor-based circuits such as super capacitors and charge pumps, which capture MFC energy passively and transfer it to a boost converter.<sup>11,12</sup> For example, a recently study by Liang et al. showed that current production from a BES reactor can be increased by 22–32% if an alternative

Received: January 26, 2012

Revised: April 5, 2012

Accepted: April 9, 2012

Published: April 9, 2012

charging and discharging method is used. In such operation, a capacitor is first charged by the reactor but then discharges the electrons back to the reactor. This is different from traditional intermittent charging, where a capacitor discharged the collected electrons to a resistor.<sup>11</sup> Another study by Kim et al., showed that parallel charging of multiple capacitors can avoid potential voltage reversal while series discharging could increase MFC output voltage.<sup>13</sup> The problem of directly using capacitors or charge pumps is that such devices can only passively receive MFC energy at a fixed operating point without any control on the MFC reactor, and the operating points cannot be adjusted to capture energy at the maximum power density point.

In this study, we developed a new energy harvesting approach and system that not only can capture the maximum power from the MFC, but also harvests energy actively without using any resistance. Instead of passively receiving electrons from the MFC reactor, this controller can actively extract energy from the MFC at any operating point, especially at the peak power point to maximize energy production. The energy harvesting efficiency, organic removal, and Coulombic efficiency of the MFC operated by this maximum power point circuit (MPPC) was characterized and compared with a common charge pump operation. The energy storage capacity using different numbers of capacitors and system energy conversion efficiency was also investigated for system optimization.

## MATERIALS AND METHODS

**MFC Construction and Operation.** Each MFC reactor consisted of two polycarbonate cube-shaped chambers that were separated by a cation exchange membrane (38 cm<sup>2</sup>, CMI-7000, Membranes International, NJ).<sup>14</sup> The empty volume of either anode or cathode chamber was 150 mL. Heat-treated graphite brushes were used as the anodes, and carbon cloth (projected surface area 38 cm<sup>2</sup>) was selected as the cathode material.<sup>15,16</sup> MFCs were inoculated with anaerobic sludge obtained from Longmont Wastewater Treatment Plant (Longmont, CO). The anode chamber was fed with growth medium containing (per liter) 1.25 g of CH<sub>3</sub>COONa, 0.31 g of NH<sub>4</sub>Cl, 0.13 g of KCl, 3.32 g of NaH<sub>2</sub>PO<sub>4</sub>·2H<sub>2</sub>O, 10.32 g of Na<sub>2</sub>HPO<sub>4</sub>·12H<sub>2</sub>O, 12.5 mL of mineral solution, and 5 mL of vitamin solution.<sup>3</sup> Phosphate buffered potassium ferricyanide solution (50 mM) was used as the catholyte to minimize the cathode effects on system performance.<sup>14</sup> MFCs were operated in fed-batch mode at the acclimation stage until repeatable voltage profiles were obtained. Reactors were then operated by recirculating anolyte with a 1000 mL reservoir at a flow rate of 45 mL/min and recirculating catholyte with another reservoir at a flow rate of 114 mL/min, respectively. Such operation was aimed to maintain stable substrate and pH conditions so energy harvesting characterization could be focused.<sup>17,18</sup>

**Maximum Power Point Circuit (MPPC) Design and Operation.** The MPPC consisted of a metal-oxide-semiconductor field-effect transistor (MOSFET), a comparator, an inductor, a diode, capacitors, potentiometers, and connectors. Detailed information on each MPPC component is listed in Figure S1 (Supporting Information), and the circuit design details are described by Park and Ren.<sup>19</sup> Figure 1 shows the principles of the energy harvesting MPPC. The MPPC is able to operate the MFC reactor in the vicinity of the maximum power operating point, which is regulated by a hysteresis controller (Figure 1A). The hysteresis controller confines the

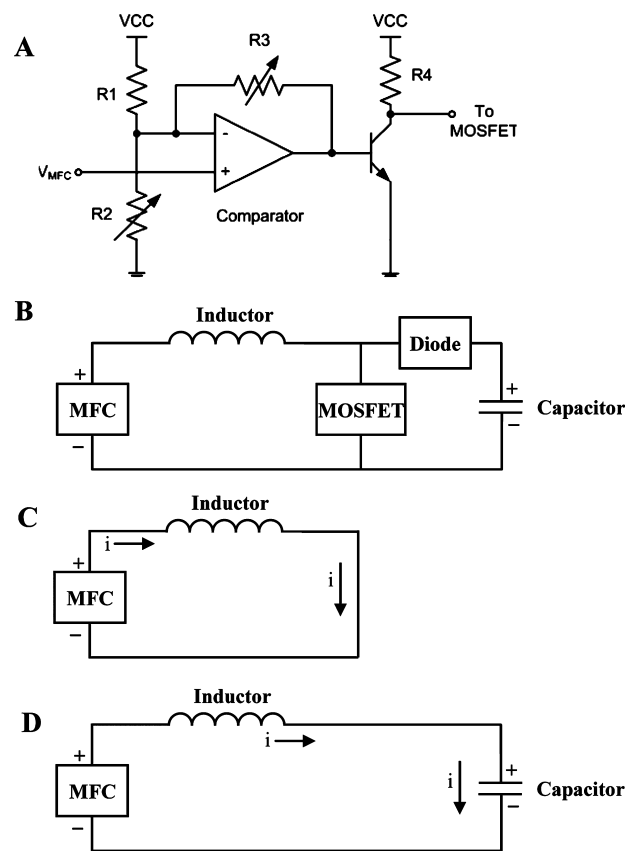


**Figure 1.** Block diagram of the maximum power point circuit (MPPC): (A) harvesting converter controller; (B) whole electric circuit diagram; (C) CHARGE phase, MOSFET is on while diode is off, extracted energy is stored in the inductor; (D) DISCHARGE phase, MOSFET is off while diode is on, extracted energy is stored in the capacitors.

MFC voltage in a predefined range to avoid voltage collapse and ensure enough recovery time of the MFC reactor, and the upper ( $V_{thH}$ ) and lower ( $V_{thL}$ ) voltage thresholds can be defined by eq 1<sup>19</sup>

$$V_{thH} = V_{cc} \frac{R_2}{R_2 + (R_1 // R_3)} \quad V_{thL} = V_{cc} \frac{R_2 // R_3}{R_2 + (R_2 // R_3)} \quad (1)$$

where  $V_{cc}$  is the external voltage for MPPC circuit,  $R_1$ ,  $R_2$ , and  $R_3$  are internal resistors to set the harvesting hysteresis voltage band, and the double slash means parallel connections of resistors (Figure 1). For comparison with traditional passive energy harvesting approaches, a charge pump (S-882Z24, Seiko Instruments) was used in a control experiment with the same reactor configuration and operation.

The operation of the MPPC consists of two modes, CHARGE and DISCHARGE, according to the energy flow on the inductor connected with the MFC (Figure 1B). During CHARGE mode, the MOSFET switch is on and diode is off, and the energy is extracted from the MFC and charged to the inductor (Figure 1C). Due to energy extraction, the voltage of the MFC decreases in this mode. During DISCHARGE mode, the MOSFET switch is off and diode is on, and the energy stored in the inductor is discharged to the capacitor (Figure 1D). MFC voltage increases in this mode as it recovers from energy extraction. The controller turns off the MOSFET automatically when the MFC voltage reaches lower threshold in

CHARGE mode and turns it back on when the MFC voltage gets to the upper threshold in DISCHARGE mode. The duty ratio and switching frequency can vary depending on the generating capacity and recovery time of the operating MFC. The comparator generated hysteresis voltage band according to the MFC voltage, and the voltage band can be easily tracked and adjusted by potentiometers.<sup>20</sup>

**Analyses.** The MFC voltage, capacitor voltage, and the output voltage across a current probe (K110, AEMC Instruments) were recorded at 66-s intervals using a data acquisition system (Keithley Instrument, OH). The anode potential and cathode potential were measured against a Ag/AgCl reference electrode (RE-5B, Bioanalysis) inserted in the anode chamber. An oscilloscope (TPS2014B, Tektronics) was used to continuously monitor MFC voltage, output current, and the main switch on/off signal. Chemical oxygen demand (COD) was measured using a standard colorimetric method (Hach Company, CO). Polarization curves were obtained by linear sweep voltammetry (LSV) using a potentiostat (PC4/300, Gamry Instruments, NJ). The scan rate of LSV was 0.1 mV/s with the anode as working electrode and the cathode as counter and reference electrode.<sup>16,21</sup>

The output power ( $P$ ) of MFC was calculated by  $P = UI$ , where  $U$  is the voltage across the MFC anode and cathode and  $I$  is the MFC output current monitored by the current meter. Power density and current density were normalized by the projected area of the cathode ( $38 \text{ cm}^2$ ). Energy ( $W_c$ ) consumed by an external resistor ( $R$ ) was calculated by  $W_c = \int U^2/Rdt$ , and the energy ( $W_p$ ) supplied by the MFC during harvesting by the MPPC or charge pump was expressed as  $W_p = \int Pd_t$ , where  $dt$  is 66 s. The energy ( $E$ ) stored in the capacitors was calculated by  $E = 0.5CV^2$ , where  $C$  is the capacitance and  $V$  is the capacitor voltage. Energy conversion efficiency ( $ECE$ ) was calculated by  $ECE = E/W_p \times D \times 100\%$ . The energy ( $J$ ) consumption in each MPPC component was calculated based on  $E = VI$  during the harvesting period. Coulombic efficiency ( $CE$ ) was presented as  $CE = 8000 \int Idt / FV\Delta COD$ , where  $F$  is Faraday constant,  $V$  is total volume, and  $\Delta COD$  is COD concentration change. Duty ratio ( $D$ ) was defined as the ratio of turn-on time to the total switching time,  $D = t_{on} / (t_{on} + t_{off})$ , where  $t_{on}$  and  $t_{off}$  are the on and off time of the MOSFET, respectively.

## RESULTS AND DISCUSSION

**MPPC Can Operate the MFC at the Maximum Power Harvesting Range.** Figure 2 shows the polarization and power density curves obtained in the steady-state recirculating flow MFC reactor. The maximum power density produced by the MFC was around  $1370 \text{ mW/m}^2$  when the reactor voltage was between 372 and 316 mV, with an average of 344 mV. The corresponding external resistor at the peak power density was  $23 \Omega$ . To harvest the maximum power identified by the MFC power density curve, the upper voltage threshold at 372 mV and lower voltage threshold at 316 mV were determined to form an energy extraction band for the hysteresis controller in MPPC. In contrast, the charge pump was only able to harvest the MFC energy at the 633 mV ( $317 \text{ mW/m}^2$ ) due to the current limitation of the charge pump (Figure 2). The difference in the operating points on the power density curve demonstrates that the MPPC could be modulated to harvest energy at the range of the peak point while the power harvesting by the charge pump was limited at lower points due to the lack of controllability.

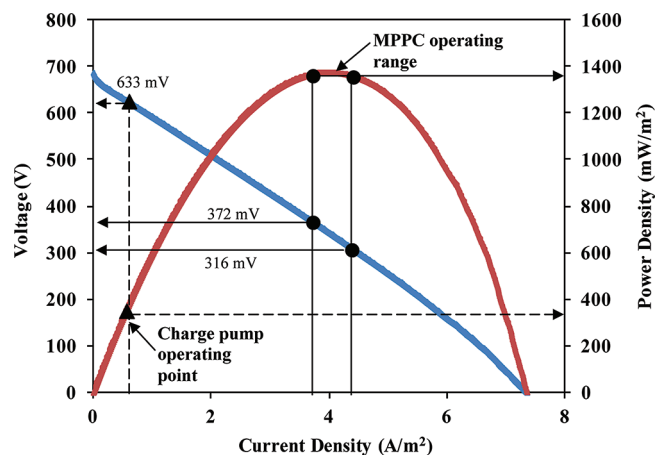


**Figure 2.** MFC polarization curve and power density curve obtained by linear sweep voltammetry (LSV). The scan rate of the polarization was 0.1 mV/s. ▲: Operating point of the charge pump. ●: Operating range of the MPPC. Recirculating-flow MFC open circuit potential was 688 mV.

Typical operation cycles of the MPPC harvesting are shown in Figure 3. When the MFC voltage reaches 372 mV, the

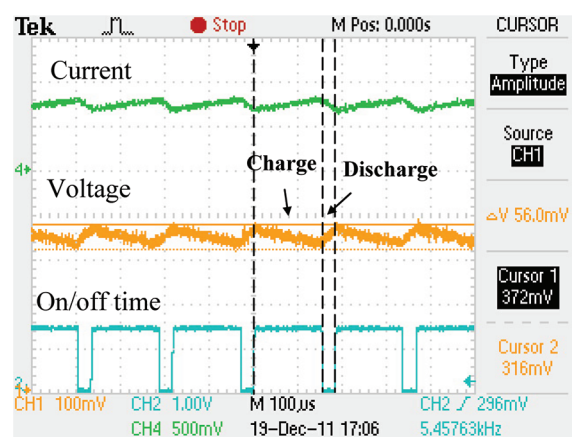


**Figure 3.** Snapshot of on/off cycle of the MPPC during active energy harvesting from MFCs and the voltage and current profiles. One division of X-axis represents  $100 \mu\text{s}$ . The figure shows the waveforms of 1 ms duration in terms of current, voltage, and on/off switch changes.

MPPC actively extracts energy from the MFC and charges the inductor (CHARGE mode). The extraction stops when the voltage drops to 316 mV. While waiting for the MFC voltage to recover, the controller discharges the energy from the inductor to the capacitor (DISCHARGE mode). Once the MFC voltage recovers back to 372 mV, the controller charges the inductor again. The switching frequency is very fast and in the order of kHz. The duration of CHARGE and DISCHARGE phases depends on the MFC condition, and the DISCHARGE phase was also affected by the target of the capacitor voltage. The range of operation can be tracked and controlled by the hysteresis controller.<sup>20</sup> Anolyte and catholyte recirculation operation was used in this study because such system could maintain a relatively stable substrate concentration, pH, and other operating conditions as compared to fed-batch operation and thus reduces the effects of environmental factors.

**MPPC Harvests Energy More Actively and Efficiently.** MFC power density curves demonstrate that when the applied external resistance is equal to the MFC internal resistance, the maximum power can be achieved. Figure 2 shows that the peak power of the MFC used in this study could be obtained at 23 Ω, and Figure 4 shows the MPPC-controlled MFC was

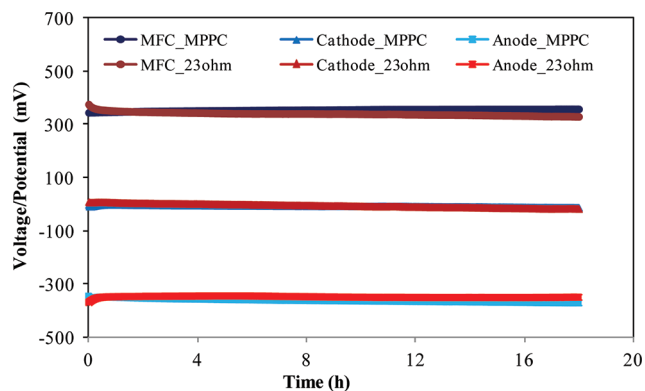


**Figure 4.** Comparison of MFC voltage, cathode potential, and anode potential between the MPPC active energy harvesting condition and 23 Ω external resistor condition. The optimum external resistance was calculated to be 23 Ω based on polarization curve that could yield the maximum power density.

operated at nearly the same condition as the reactor operated under a 23 Ω resistor. The operating curves of the anode potential, cathode potential, and reactor voltage in both conditions basically overlapped each other, indicating very similar operating conditions, where the maximum power could be generated. However, instead of dissipating the energy into heat as resistors do, the MPPC captured the energy and stored energy into capacitors.

Energy harvesting results show that the MPPC-controlled MFC was able to charge multiple capacitors (Taiyo Yuden, PAS1016LR2R3205). After 18 h of operation, the voltage of the 12 capacitors connected to the MPPC controller increased from 0 to 2.5 V, and the MPPC extracted 214.1 J of energy from the MFC, in which 76.8 J was stored in the capacitors (Figure 5A). In comparison, the charge pump was able to charge 1 capacitor to 1.0 V during the same period, and the total extracted and stored energy was 23.2 and 1.0 J,

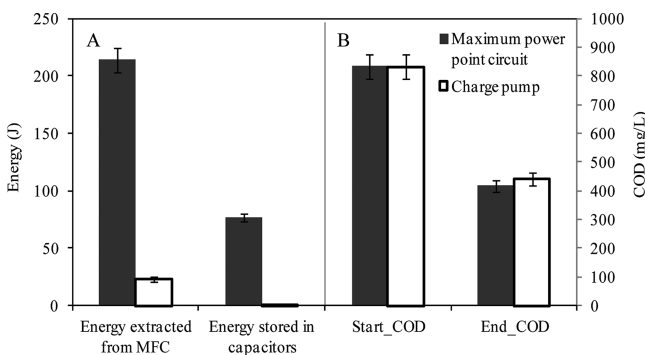


**Figure 5.** (A) Comparison of energy harvesting by the MPPC and the charge pump and energy stored in capacitors. (B) Comparison of COD removals in the MPPC and charge pump conditions. In the MPPC test, 12 capacitors were connected in parallel for energy storage. In the charge pump test, one capacitor was enough to store all the harvested energy from MFC.

respectively (Figure 5A). The results show that by actively extracting energy at the maximum power point, the MPPC harvested 76 times more energy than the charge pump.

Comparable substrate degradation was observed in both energy harvesting operations, as the COD removals were 49.8% and 47.1% for the MPPC and charge pump, respectively (Figure 5B). However, the Coulombic efficiency of the MPPC operation was 15.6%, 21 times higher than that of the charge pump (0.7%). This finding is consistent with previous studies that higher Coulombic efficiency can be achieved by operating MFCs at an optimal external resistance.<sup>5</sup> Moreover, compared to other studies that selected the optimal resistance to demonstrate the power generation potential, the MPPC actually captured the energy at the maximum power point that is available for electronic utilization. Ferricyanide solution was used as the catholyte in this 2-chamber MFC study, so no cathode biofilm was observed to consume substrate and affect Coulombic efficiency.

**Numbers of Capacitors for Energy Storage.** Different numbers of capacitors were tested in the study for energy storage and to provide stable electricity for electronic devices. While resistors do not capture any energy, and the charge pump was only able to charge 1 capacitor, the MPPC harvested so much energy that multiple capacitors had to be used for energy storage. The charging behavior of using 3, 6, 9, and 12 capacitors during 18-h harvesting was characterized. The capacitors were connected in parallel in order to maintain charging efficiency. Figure 6 shows that with the increase of charging time, the voltage of the 3-capacitor condition increased faster than other conditions and reached the saturated level of 2.9 V in 4 h. The stored energy in the 3 capacitors was 25.2 J within this period. After 4 h, the 3-capacitors could not store more energy due to saturation, but the MPPC kept

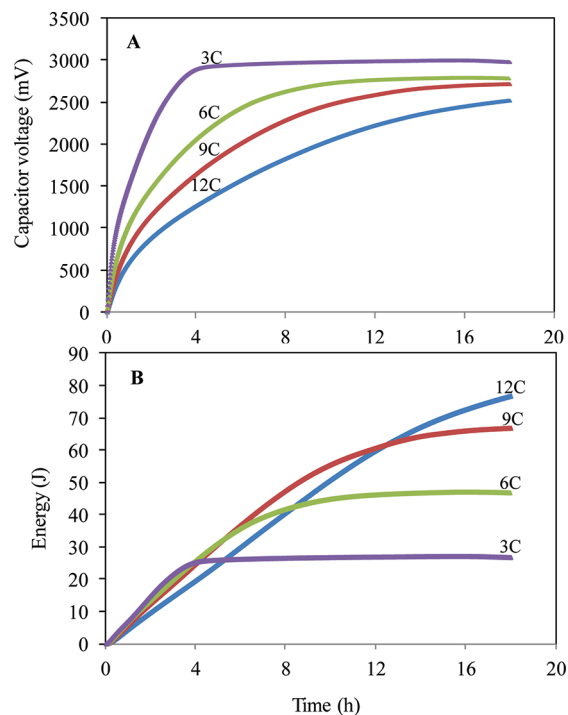


**Figure 6.** (A) Voltage profile and (B) energy storage differences by using 3, 6, 9, and 12 capacitors in parallel during MPPC active energy harvesting.

harvesting energy from the MFC, as evidenced by the 6, 9, and 12-capacitor conditions. With increasing numbers of capacitors, the voltage increase rate declined, but the total amount of energy stored in capacitors increased. The energy storage in the 6, 9, and 12-capacitor conditions was 47.0, 65.6, and 76.8 J, respectively, and the corresponded voltage after 18 h was 2.8, 2.7, and 2.5 V, respectively. Because the larger the capacitance, the longer the charging time is required, which resulted in differences in capacitor voltages and energy storage. More energy can be stored in higher capacitance conditions if the harvesting continues. These results indicate that different numbers of capacitors or capacitors with different capacitance can be used as energy storage for operating electronic devices. The required number of capacitors, charging time, and energy storage capacity are determined by the characteristics of end users, and the MPPC-controlled MFC should not be a limiting factor under stable operating condition.

**Conversion Efficiency of the MPPC.** The MPPC can actively harvest energy at the maximum power point thus significantly increased energy generation from MFCs. However, like any electronic device, the MPPC consists of multiple electronic components that consume energy, which reduce MPPC's energy conversion efficiency. When the MFC was operated under  $23 \Omega$ , the optimal external resistance that led to the maximum power density, the MFC could provide 215.7 J (prorated by duty ratio) of energy in 18 h, even though all such energy will be dissipated through heat by the resistor. In comparison, the MPPC harvested 214.1 J of energy from the MFC without external resistors and transferred 76.8 J to the capacitors. This further confirmed that the MPPC was able to harvest 99.2% of the energy from the MFC, but it also shows that only 35.9% of the harvested energy was transferred to the capacitors. Even though the MPPC-transferred energy is still 76 times higher than that from the charge pump (1.0 J), it is important to identify the limiting factors within the MPPC circuit and improve the conversion efficiency. Figure S2 shows the MPPC efficiency through an 18-h test, and it can be seen that the efficiency increased sharply at the beginning and then stabilized until a decline was observed due to the saturation of capacitance. The highest energy extraction efficiencies occurred between 8.3 and 11.5 h, with an efficiency of 42.1%. The power consumption of each component in the MPPC circuit was calculated in Table S1 (Supporting Information). Figure 7 illustrates the percentage of energy loss in each component during MFC energy extraction by the MPPC during an 18-h period. While most MPPC components consumed minimum

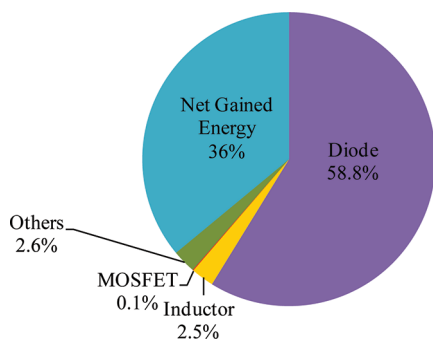


**Figure 7.** Energy conversion efficiency and distribution of internal energy loss in the MPPC. The distribution was quantified based on an 18-h, 12-capacitor operation.

amount of energy, the diode contributed to 58.8% of the energy loss within the MPPC, indicating that it is the single element that needs to be replaced or improved. The diode is used in the MPPC to transfer the energy from the inductor to capacitors and blocks reverse flow. Advanced converters are currently being developed to replace the diode and improve MPPC conversion efficiency.

## OUTLOOK

MFC technology has been considered as a sustainable method to directly produce energy from biodegradable substrates, but the improvement of power density has been stagnant for several years after significant advancements in reactor configuration and material development. Compared with traditional approaches that use external resistors and charge pumps, this study demonstrates a new active approach to harvest energy from MFCs. Instead of passively receiving electrons from the MFC, the MPPC actively extracts energy from the MFC at the peak power point. The remarkable increase in energy generation by the MPPC compared to the common charge pump shows this approach is much more efficient and effective to capture MFC energy. There are very few charge pumps available for MFC systems, and the charge pump used in this study is representative, because it has been used by many other studies in different conditions.<sup>22–24</sup>

The active energy harvesting approach is new to MFC operation, and there are many questions that remain to be answered. For example, one unique feature of MFCs is the variable biocatalyst density on the electrodes. Exoelectrogenic bacteria transfer electrons to the anode electrode and gain energy during anaerobic respiration. Within the capability of bacterial extracellular electron transfer, the more electrons that get extracted from the external circuit, the less electrons and energy become available for microbial growth. Therefore, it is important to understand how the active harvesting affects microbial activity, community, and metabolisms, so a balanced and sustainable reactor performance can be maintained. We did not find active harvesting negatively affecting MFC performance in terms of power density and Coulombic efficiency in recirculation operation. In addition, further optimization of the MPPC circuit needs to be conducted to reduce internal energy loss. Systems with precise tracking capability will allow the circuit to adjust and maintain the maximum energy extraction based on real-time changes of MFC condition due to the variations of environmental conditions such as pH, temperature, and substrate concentration.

## ASSOCIATED CONTENT

### Supporting Information

Two additional figures and one table. This material is available free of charge via the Internet at <http://pubs.acs.org>.

## AUTHOR INFORMATION

### Corresponding Author

\*E-mail: [zhijong.ren@ucdenver.edu](mailto:zhijong.ren@ucdenver.edu); phone: (303) 556-5287; fax: (303) 556-2368.

### Notes

The authors declare no competing financial interest.

## ACKNOWLEDGMENTS

This work was supported by the Office of Naval Research (ONR) under Award N000140910944. We thank Drs. Bruce Logan and Peter Jenkins for constructive discussions.

## REFERENCES

- (1) Fan, Y. Z.; Sharbrough, E.; Liu, H. Quantification of the Internal Resistance Distribution of Microbial Fuel Cells. *Environ. Sci. Technol.* **2008**, *42* (21), 8101–8107.
- (2) Logan, B. E. Scaling up microbial fuel cells and other bioelectrochemical systems. *Appl. Microbiol. Biotechnol.* **2010**, *85* (6), 1665–1671.
- (3) Ren, Z.; Yan, H.; Wang, W.; Mench, M.; Regan, J. Characterization of microbial fuel cells at microbially and electrochemically meaningful timescales. *Environ. Sci. Technol.* **2011**, *45* (6), 2435–2441.
- (4) Wagner, R. C.; Call, D. F.; Logan, B. E. Optimal set anode potentials vary in bioelectrochemical systems. *Environ. Sci. Technol.* **2010**, *44* (16), 6036–6041.
- (5) Pinto, R. P.; Srinivasan, B.; Guiot, S. R.; Tartakovsky, B. The effect of real-time external resistance optimization on microbial fuel cell performance. *Water Res.* **2011**, *45* (4), 1571–1578.
- (6) Biffinger, J. C.; Pietron, J.; Bretschger, O.; Nadeau, L. J.; Johnson, G. R.; Williams, C. C.; Neelson, K. H.; Ringeisen, B. R. The influence of acidity on microbial fuel cells containing *Shewanella oneidensis*. *Biosens. Bioelectron.* **2008**, *24* (4), 906–911.
- (7) He, Z.; Huang, Y.; Manohar, A. K.; Mansfield, F. Effect of electrolyte pH on the rate of the anodic and cathodic reactions in an air-cathode microbial fuel cell. *Bioelectrochemistry* **2008**, *74* (1), 78–82.
- (8) Cheng, S. A.; King, D. F.; Logan, B. E. Electricity generation of single-chamber microbial fuel cells at low temperatures. *Biosens. Bioelectron.* **2011**, *26* (5), 1913–1917.
- (9) Liu, H.; Cheng, S.; Logan, B. E. Production of electricity from acetate or butyrate using a single-chamber microbial fuel cell. *Environ. Sci. Technol.* **2005**, *39* (2), 658–662.
- (10) Woodward, L.; Perrier, M.; Srinivasan, B.; Pinto, R. P.; Tartakovsky, B. Comparison of Real-Time Methods for Maximizing Power Output in Microbial Fuel Cells. *AIChE J.* **2010**, *56* (10), 2742–2750.
- (11) Liang, P.; Wu, W.; Wei, J.; Yuan, L.; Xia, X.; Huang, X. Alternate charging and discharging of capacitor to enhance the electron production of bioelectrochemical systems. *Environ. Sci. Technol.* **2011**, *45* (15), 6647–6653.
- (12) Donovan, C.; Dewan, A.; Heo, D.; Beyenal, H. Batteryless, Wireless Sensor Powered by a Sediment Microbial Fuel Cell. *Environ. Sci. Technol.* **2008**, *42* (22), 8591–8596.
- (13) Kim, Y.; Hatzell, M. C.; Hutchinson, A. J.; Logan, B. E. Capturing power at higher voltages from arrays of microbial fuel cells without voltage reversal. *Energy Environ. Sci.* **2011**, *4* (11), 4662–4667.
- (14) Luo, H.; Xu, P.; Roane, T. M.; Jenkins, P. E.; Ren, Z. Microbial desalination cells for improved performance in wastewater treatment, electricity production, and desalination. *Bioresour. Technol.* **2012**, *105*, 60–66.
- (15) Wang, X.; Cheng, S. A.; Feng, Y. J.; Merrill, M. D.; Saito, T.; Logan, B. E. Use of Carbon Mesh Anodes and the Effect of Different Pretreatment Methods on Power Production in Microbial Fuel Cells. *Environ. Sci. Technol.* **2009**, *43* (17), 6870–6874.
- (16) Wang, H.; Wu, Z.; Plaseied, A.; Jenkins, P.; Simpson, L.; Engtrakul, C.; Ren, Z. Carbon nanotube modified air-cathodes for electricity production in microbial fuel cells. *J. Power Sources* **2011**, *196* (18), 7465–7469.
- (17) Luo, H.; Jenkins, P.; Ren, Z. Concurrent desalination and hydrogen generation using microbial desalination cells. *Environ. Sci. Technol.* **2011**, *45* (1), 340–344.
- (18) Zhang, F.; Jacobson, K.; Torres, P.; He, Z. Effects of anolyte recirculation rates and catholytes on electricity generation in a liter-scale upflow microbial fuel cell. *Energy Environ. Sci.* **2010**, *3*, 1347–1352.
- (19) Park, J.; Ren, Z. Efficient Energy Harvester for Microbial Fuel Cells using DC/DC Converters. In *Proceedings of IEEE Energy Conversion Congress and Exposition*, 2011; pp 3852–3858.
- (20) Park, J. D.; Ren, Z. Y. Hysteresis Controller Based Maximum Power Point Tracking Energy Harvesting System for Microbial Fuel Cells. *J. Power Sources* **2012**, *205* (9), 151–156.
- (21) Zhang, F.; Saito, T.; Cheng, S.; Hickner, M.; Logan, B. Microbial fuel cells cathodes constructed from stainless steel mesh that use poly(dimethylsiloxane) diffusion layers. *Environ. Sci. Technol.* **2010**, *44* (4), 1490–1495.
- (22) Meehan, A.; Gao, H.; Lewandowski, Z. Energy Harvesting with Microbial Fuel Cell Power Management System. *IEEE Trans. Power Electron.* **2011**, *26* (1), 176–181.
- (23) Donovan, C.; Dewan, A.; Peng, H.; Heo, D.; Beyenal, H. Power Management System for a 2.5W Remote Sensor Powered by a Sediment Microbial Fuel Cell. *J. Power Sources* **2011**, *196* (3), 1171–1177.
- (24) Zhang, F.; Tian, L.; He, Z. Powering a wireless temperature sensor using sediment microbial fuel cells with vertical arrangement of electrodes. *J. Power Sources* **2011**, *196* (22), 9568–9573.